

# A New Grid of Model Atmospheres for Metal-poor Ultracool Brown Dwarfs

Roman Gerasimov<sup>1</sup> , Derek Homeier<sup>2</sup> , Adam Burgasser<sup>1</sup> , and Luigi R. Bedin<sup>3</sup>

Published December 2020 • © 2020. The American Astronomical Society. All rights reserved.

Research Notes of the AAS, Volume 4, Number 12

**Citation** Roman Gerasimov *et al* 2020 *Res. Notes AAS* **4** 214

---

romang@ucsd.edu

romang@ucsd.edu

<sup>1</sup> Center for Astrophysics and Space Sciences University of California, San Diego, La Jolla, California 92093, USA; romang@ucsd.edu

<sup>2</sup> Förderkreis Planetarium Göttingen, Germany

<sup>3</sup> INAF-Osservatorio Astronomico di Padova, Vicolo dell'Osservatorio 5, I-35122 Padova, Italy

Roman Gerasimov  <https://orcid.org/0000-0003-0398-639X>

Derek Homeier  <https://orcid.org/0000-0002-8546-9128>

Adam Burgasser  <https://orcid.org/0000-0002-6523-9536>

Received November 2020

Accepted November 2020

Published December 2020

<https://doi.org/10.3847/2515-5172/abcf2c>

Stellar atmospheres; Brown dwarfs; Stellar abundances

 [Journal RSS](#)

[Sign up for new issue notifications](#)

[Create citation alert](#)

## Abstract

This site uses cookies. By continuing to use this site you agree to our use of cookies. To find out more, see our [Privacy and Cookies policy](#).



We present a new grid of model atmospheres and synthetic spectra down to extremely metal-poor ( $[\text{M}/\text{H}] \geq -3.0$ ), ultracool ( $T_{\text{eff}} \geq 900$  K) brown dwarfs based on the PHOENIX code (Hauschildt et al. 1997). The grid is publicly available and continuously updated as new models are computed. The models are aimed at characterizing metal-poor halo brown dwarfs identified in surveys such as Backyard Worlds: Planet 9 (Kuchner et al. 2017; Schneider et al. 2020) and brown dwarfs in globular clusters (Dieball et al. 2019). Our setup includes the formation and depletion by gravitational settling of condensate clouds as defined for the BT-Settl grid of Allard et al. (2012), using the version 15.5 branch of PHOENIX, which was split off from the main branch (Barman et al. 2011; Husser et al. 2013). Our calculations employ the Allard & Homeier cloud formation model (Helling et al. 2008; Allard et al. 2012).

Export citation and abstract

[BibTeX](#)

[RIS](#)

[◀ Previous article in issue](#)

[Next article in issue ▶](#)

---

Model atmospheres are stratified into 250 isotropic layers. Radii are adopted from the best-matching cooling models of Baraffe et al. (2015). The initial pressure-temperature profile is extracted from either the closest NextGen<sup>4</sup> model or, for cooler models and in cases of convergence issues, from a previously calculated model in our grid with similar parameters. We use the equation of state from Allard et al. (2001) to compute partial pressures for  $\sim 500$  gaseous and  $\sim 200$  condensate species, with chemical equilibrium constants drawn mostly from Chase (1986); Sharp & Huebner (1990). We adopt elemental abundances<sup>5</sup> from Caffau et al. (2011a, 2011b) and Asplund et al. (2009), scaled by metallicity with enhancements of individual elements as necessary. For liquid or solid species that are depleted from the atmosphere by settling/rainout, the abundances of corresponding elements are removed from the condensation layer and all layers above.

PHOENIX converges on a self-consistent atmosphere iteratively. The composition of each layer is computed under stationary equilibrium, with possible modifications to incorporate diffusive mixing as detailed below. Corresponding opacities are sampled at  $\sim 100,000$  wavelengths spanning  $1\text{\AA}$  to  $1\text{mm}$ , with a median resolution of  $\lambda/\Delta\lambda \approx 18250$  in the range  $0.4$

This site uses cookies. By continuing to use this site you agree to our use of cookies. To find out more, see our Privacy and Cookies policy. 

transitions from Kurucz (1995), and  $0.6 \times 10^9$  molecular transitions from multiple sources.<sup>6</sup> Approximately 20% of these transitions correspond to less than  $10^{-6}$  of the continuum flux and are discarded. Depending on the strength of the line, Doppler or Voigt profiles are used to model the contribution of each transition. We deploy standard damping constants for the Lorentz wings for most transitions (e.g., Barklem & O'Mara 1997), but for select atomic species (H<sub>I</sub>, He<sub>I</sub>, Na<sub>I</sub>, K<sub>I</sub>, Li<sub>I</sub>, Ca<sub>I</sub>, Ca<sub>II</sub>, Rb<sub>I</sub>, Cs<sub>I</sub>) these profiles are computed using pressure-broadening profiles following Allard & Spiegelman (2006), Allard et al. (2007, and references therein). At the end of each iteration, energy conservation is used to update the temperature structure (Dreizler 2003). Iterations are repeated until no further improvement can be made. A typical model requires  $\sim 100$  iterations to converge, and takes  $\sim 100$  CPU hours on the XSEDE Comet cluster (Towns et al. 2014).

Convective energy transfer is modeled using Mixing-Length Theory (Böhm-Vitense 1958; Smalley 2005) for any superadiabatic layers occurring at  $\log_{10}(\tau) > -2$ . The mixing length is set to  $\approx 2$  pressure scale heights, as required to reproduce the average pressure-temperature profiles from 2D and 3D radiative hydrodynamic simulations (Freytag et al. 2010, 2013; see Baraffe et al. 2015 for a discussion). While the contribution to energy transfer from overshoot above the Schwarzschild boundary is ignored in this approach, our models include the contribution of overshoot to the velocity field, assuming an exponential decay of the turbulent velocity field with a gravity and temperature-dependent scale height. We also include the mixing contribution of gravity waves excited by convection following Freytag et al. (2013). The resulting vertical mixing contributes to departures from local thermochemical equilibrium, particularly for nitrogen (N<sub>2</sub>, NH<sub>3</sub>) and carbon species (CO, CO<sub>2</sub>, CH<sub>4</sub>; see Visscher et al. (2010) for the relevant reaction networks and rates), and sets the balance between grain growth and sedimentation of condensate particles.

The microturbulent velocity adopted for Doppler line broadening is allowed to scale linearly with temperature from  $\sim 0.1 \text{ km s}^{-1}$  at 2000K to  $\sim 0.4 \text{ km s}^{-1}$  at 4000K, following Husser et al. (2013). The velocity is fixed at  $\sim 0.1 \text{ km s}^{-1}$  in the coldest atmospheres. The convective mixing velocity is added in quadrature to the microturbulent motion to calculate the Doppler broadening of atomic and molecular lines.

In our models, 200 condensate species ("dust") are allowed to condense into "clouds" under appropriate thermochemical conditions, with the lower cloud boundaries defined by the sublimation/condensation temperatures. The vertical extent is modeled in the Settl approach. This site uses cookies. By continuing to use this site you agree to our use of cookies. To find out more, see our [Privacy and cookies policy](#).

growth and sedimentation rates of dust due to gravitational settling. Sedimentation is particularly important at  $T_{\text{eff}} \lesssim 2000\text{K}$ , marking the transition from "dusty" atmospheres that are dominated by cloud opacity to "cloudy" atmospheres that feature thinner and deeper cloud layers due to gravitational settling. Clouds also deplete the abundances of the constituent elements, reducing the gas opacity, while contributing additional scattering and absorption opacity. The latter is calculated for the 10 most important condensates in each layer. Dust grains are assumed to be pure and non-porous, with a log-normal distribution of grain sizes with a mean calculated from the balance of mixing, growth, and settling for each layer, and distribution width of  $\sigma = 1.0\text{dex}$ . Wavelength-dependent absorption and extinction coefficients for the individual species are calculated from the optical constants using Mie and Rayleigh theory. Clouds are assumed to cover the entire surface of the star uniformly.

We maintain an online repository of the models,<sup>7</sup> including atmospheric pressure-temperature profiles and synthetic spectra. Figure 1 provides example models for a range of temperatures and metallicities.

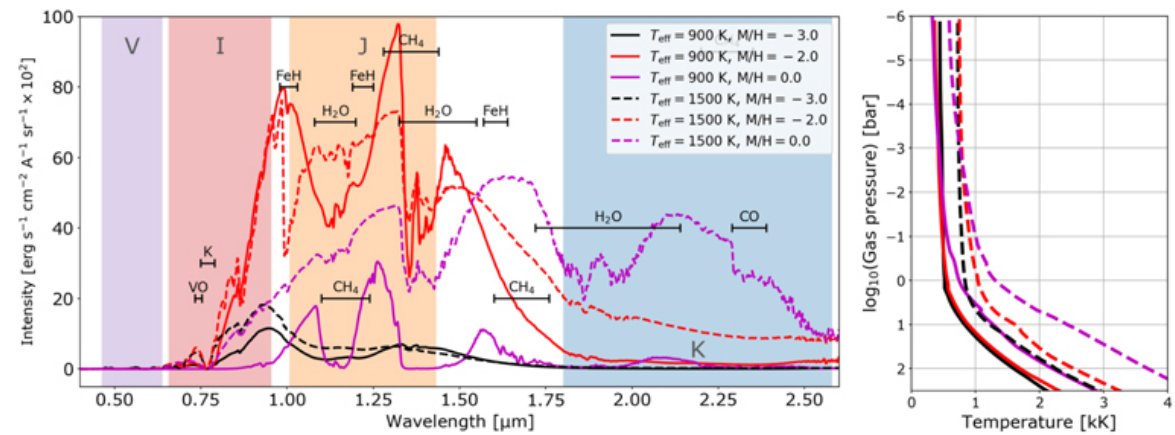


**Figure 1.** Representative atmosphere models from our metal-poor brown dwarf grid. Left: synthetic spectra of selected models available in the repository. Some absorption bands from important species are labeled. The spectral bands covered by standard *V*, *I*, *J*, and *K* filters are indicated by color shading. Right: corresponding pressure-temperature profiles.

X.S.E.D.E. is supported by NSF grant ACI-1548562. R.G. and A.B. acknowledge support from HST GO-15096. I.R.B. acknowledges support from PRIN-MIUR #2017Z2HSMF. This site uses cookies. By continuing to use this site you agree to our use of cookies. To find out more, see our Privacy and Cookies policy.



## Footnotes

4 [phoenix.ens-lyon.fr/Grids/NextGen](http://phoenix.ens-lyon.fr/Grids/NextGen)

5 [atmos.ucsd.edu/?p=solar](http://atmos.ucsd.edu/?p=solar)

6 [atmos.ucsd.edu/?p=molecular](http://atmos.ucsd.edu/?p=molecular)

7 [atmos.ucsd.edu](http://atmos.ucsd.edu)

---

